Available online at www.sciencedirect.com
SCIENCE DIRECT®
Estuarine, Coastal and Shelf Science 68 (2006) 195–207
ESTUARINE COASTAL AND SHELF SCIENCE
www.elsevier.com/locate/ecss

A heuristic formula for turbulence-induced flocculation of cohesive sediment

J.C. Winterwerp [a,b,*], A.J. Manning [c,d], C. Martens [e], T. de Mulder [f], J. Vanlede [f]

[a] *Delft Hydraulics, PO Box 177, 2600 MH Delft, The Netherlands*
[b] *Delft University of Technology, Delft, The Netherlands*
[c] *Centre for Coastal Dynamics and Engineering (C-CoDE), Coastal Processes Research Group, School of Earth, Ocean & Environmental Sciences, University of Plymouth, Portland Square Building, Plymouth, Devon, PL4 8AA, UK*
[d] *HR Wallingford Ltd, Estuaries & Dredging group, Howbery Park, Wallingford, Oxon, OX10 8BA, UK*
[e] *International Marine & Dredging Consultants IMDC, Wilrijkstraat 37-45, B-2140, Antwerpen, Belgium*
[f] *Flanders Hydraulics Research, Berchemlei 115, B-2140, Antwerp, Belgium*

Received 3 November 2005; accepted 6 February 2006
Available online 18 April 2006

Abstract

This paper presents new measurements on the settling velocity of mud flocs in the Lower Sea Scheldt, Belgium, and compares the results with data obtained previously in the Tamar estuary, UK. The data show that the flocs are fairly compact with a fractal dimension of about 2.2, which is indicative for reaction limited aggregation processes, characteristic in dynamic aquatic systems with large tidal flow velocities and high SPM (suspended particulate matter) concentrations. The data also reveal a fairly small dependency of the settling velocity from SPM concentrations, consistently much smaller than earlier data published in literature.

Furthermore, a simple explicit formulation is proposed for the settling velocity of cohesive sediment in estuaries and coastal seas. It is derived from an analytical solution of a Lagrangean flocculation model, which accounts for turbulence-induced aggregation and floc break-up. Also the effects of variations in SPM and of a limited residence time of the flocs in the turbulent water column are included.

The model has been calibrated against data from settling velocity measurements carried out in the Tamar estuary. Values of the measured settling velocity vary between 0.5 and 5 mm s^{-1} at SPM-values between 0.05 and 8 g l^{-1}. Using the tuned coefficients, the model describes the observations satisfactory, with an overall relative standard deviation of 30%. Also, the well-known and observed increase in settling velocity with turbulent shear stress at low stresses and the opposite trend at high stresses is described properly. Next, the model is applied to the new data obtained in the Lower Sea Scheldt estuary, again comparing favourably with overall relative standard deviations of 30–50%. It appeared that the coefficients of the model can be determined from independent measurements, but two of them have to be determined by trial and error, for which a simple procedure is proposed.

Keywords: cohesive sediment; settling velocity; flocculation model; sediment transport modelling

1. Introduction

The recent increase in world trade in general and in container shipment in particular necessitates an extension of harbour basins and key walls of the Port of Antwerp, Belgium. For this purpose, the Deurganckdok is under construction, a 4500×500 m^2 basin with open connection to the Lower Sea Scheldt. As this basin is located near the turbidity maximum of the estuary, the authorities need three-dimensional sediment transport models to assess and manage the fine sediment dynamics in the estuary, amongst which assessment of volumes of maintenance dredging, the environmental impact of dumping of dredged material, etc. Therefore, the Flemish

* Corresponding author. Delft Hydraulics, PO Box 177, 2600 MH Delft, The Netherlands.
E-mail address: han.winterwerp@wldelft.nl (J.C. Winterwerp).

0272-7714/$ - see front matter © 2006 Elsevier Ltd. All rights reserved.
doi:10.1016/j.ecss.2006.02.003

government initiated an extensive program of model development and field work, the latter to collect data to determine sediment properties and data to calibrate the models under development. In this paper, we focus on one aspect of the model development and field work, i.e. the behaviour of the settling velocity of the sediment and a formulation describing its variations with shear stress, SPM (suspended particulate matter) concentration and residence time in the water column.

The transport and fate of fine suspended sediment in open, natural water systems, such as rivers, estuaries, coastal areas and oceans is governed to a large extent by the settling velocity of the sediment particles. For non-cohesive sediment, e.g. sand, this settling velocity is a unique function of the particle's diameter, its shape and the water viscosity, and can be determined straightforward with large accuracy. However, for cohesive sediment this is not the case, as the sediment is clustered in porous flocs of varying size and an ever varying composition of clay particles, silt, sometimes fine sand, organic material and a lot of water.

In low-energetic conditions at low SPM concentration, such as met in many rivers, the sediment is flocculated, but floc size and composition are fairly constant, as the flocculation time at these hydro-sedimentological conditions is quite large, e.g. Winterwerp and Van Kesteren (2004) and Winterwerp (2005).

In high-energetic conditions at high SPM concentration, such as met in many estuaries and coastal seas, floc size and composition may change continuously (Krone, 1984). This was depicted by Dyer (1989) in a conceptual diagram suggesting that floc size changes with SPM-values and turbulent shear. At low shear rates, the floc size increases with shear rate, whereas at larger shear rates, the opposite trend is expected. This diagram motivated many researchers to carry out detailed studies on the flocculation behaviour of cohesive sediment, which necessarily has to be carried out in elaborative field studies, because of the large fragility of the flocs. This, in turn, required the development of instruments for in-situ monitoring of the flocs.

One such instrument, INSSEV (IN-Situ SEttling Velocity) was developed by Fennessy et al. (1994), and has been used extensively by Manning (2001, 2004a,b). On the basis of large data sets in macrofloc ($D > 160\ \mu m$) and microfloc ($D < 160\ \mu m$) settling velocity, together with the relative floc mass distribution, Manning (2004c) derived empirical relations between the settling velocity of flocs and SPM-values and turbulent shear rate, following Dyer's diagram.

Winterwerp (1998) reasoned that the ascending branch of Dyer's diagram at low shear rates should be attributed to non-equilibrium conditions. In this phase of the flocculation process, the flocculation time is larger than the residence time of the flocs in the turbulent water column, as a result of which equilibrium floc sizes cannot be attained, contrary to the right part of the diagram where the flocculation time is short because of the large shear rates. Winterwerp (1998, 2002) developed a three-dimensional flocculation model, which indeed depicts this behaviour. However, using this model is too time-consuming to be used in operational models, and therefore parameterization is necessary to obtain an algebraic formulation that can be applied efficiently in three-dimensional sediment transport models.

In this paper, such a parameterization is proposed, based on the flocculation model by Winterwerp (1998, 2002). The underlying derivation is presented in Section 2 of this manuscript. The model is calibrated against an extensive data set from the Tamar estuary and the sensitivity of the model to the physical parameters is discussed. Section 3 describes the field campaign in the Lower Sea Scheldt and the INSSEV instrument to measure settling velocity, and presents the major data on settling velocity and relevant parameters obtained during the survey. In Section 4 the model is applied to the new data from the Lower Sea Scheldt estuary. Section 5 presents a brief discussion on the results of the measurements and the applicability of this new flocculation model. We note that this paper deals with the physical forcing of flocculation. The effects of biology in general, and of secretions by algae and bacteria, such as EPS and TEP are not treated explicitly; for state-of-the-art reviews, the reader is referred to Droppo et al. (2005). However, it has been indicated where and how these effects may be accounted for in the parameters of the flocculation model proposed.

2. A heuristic flocculation formula

2.1. Derivation of the flocculation model

The basis of the flocculation formula proposed in this paper is the three-dimensional flocculation model described in Winterwerp (2002) and its Lagrangean form (Winterwerp, 1998). This model describes flocculation as the result of turbulence-induced aggregation and floc break-up. The latter two processes work continuously, and at equilibrium, they balance. The model has one characteristic floc size, which can be regarded as the median floc size. We apply fractal theory to relate floc size and density, hence to establish the relation between floc size and settling velocity. The fractal dimension n_f is a function of sediment and water properties. If the particles stick easily upon collision, as is the case of very cohesive minerals, high organic content and/or biological activity (''diffusion limited regime''), large porous flocs are formed and n_f is small, as low as 1.7 (e.g. Vicsek, 1992; Wolanski et al., 2000). If on the other hand the flocculation processes are governed by the collision rate, as is the case in dynamic aquatic systems at high SPM concentrations (''reaction limited regime''), small, dense flocs are formed and n_f amounts to 2.2 to 2.3. A typical mean value of $n_f \approx 2$ has been found (Winterwerp, 1998).

We start the parameterization with the Lagrangean flocculation model (e.g. Winterwerp, 1998, 2002):

$$\frac{dD_f}{dt} = \frac{k_A}{n_f} c G D_f^{4-n_f} - \frac{k_B}{n_f} G^{q+1} \left(D_f - D_p\right)^p D_f^{2q+1} \tag{1}$$

in which D_f is the floc size (or its median diameter), D_p is the diameter of the primary particles from which the flocs are formed, n_f is the fractal dimension of the flocs, c is the

suspended sediment concentration by mass, and $G(\equiv\sqrt{\varepsilon/\nu}=\nu/\lambda_0^2)$ the shear rate at the smallest turbulence length scales (e.g. the Kolmogorov length scale λ_0, $\varepsilon=$ dissipation rate and $\nu=$ kinematic viscosity). Further, a dimensional aggregation parameter $k_A\left[\mathrm{m}^{n_f}\mathrm{kg}^{-1}\right]$ and floc break-up parameter $k_B\left[\mathrm{s}^{1/2}\mathrm{m}^{n_f-4}\right]$ have been defined. These parameters should be related to the physical–chemical–biological properties of the sediment and pore water (Winterwerp, 1998). However, explicit relations are not known at present, and they are therefore basically empirical coefficients. Also the coefficients p and q have to be determined from experimental data.

If we assume that $D_f \gg D_p$, the equilibrium floc size D_e follows from Eq. (1):

$$D_e^{n_f+p+2q-3}=\frac{k_A c}{k_B G^q}. \tag{2}$$

Furthermore, we assume that:

- The equilibrium floc size D_e scales with the Kolmogorov scale $D_e \propto \lambda_0$, which implies $D_e \propto G^{-1/2}$, so that:

$$n_f+p-3=0,\ \text{hence: } D_e^{2q}=\frac{k_A c}{k_B G^q} \tag{3}$$

and

- The equilibrium settling velocity $W_{s,e}$ scales with c according to:

$$W_{s,e}=W_{s,ref}\left(1+\frac{c}{c_{ref}}\right)^m \text{ which for } c\gg c_{ref} \text{ becomes: } W_{s,e}\propto c^m. \tag{4}$$

From fractal theory, one can show that $W_s \propto D_f^{n_f-1}$ (Kranenburg, 1994; Winterwerp, 1998), hence:

$$D_e^{n_f-1}\propto c^m \tag{5}$$

whence:

$$q=\frac{n_f-1}{2m}. \tag{6}$$

So we can rewrite Eq. (1) as:

$$\frac{dD_f}{dt}=\frac{k_B G^{q+1} D_f^{p+1}}{n_f}\left[D_e^{2q}-D_f^{2q}\right]. \tag{7}$$

The relevant time scale for flocculation $T'=\mathrm{F}\{n_f/k_B G^{q+1} D_f^{p+1}; D_e; D_f\}$ is an important parameter in the flocculation behaviour in estuaries and coastal seas (e.g. Winterwerp, 1998). Flocs settle continuously due to gravity and are remixed by turbulence. Hence, they experience varying hydrodynamic conditions (shear rates) during their journey through the water column. This implies that the ratio between flocculation and residence time in a specific turbulent environment becomes an important parameter.

The effects of a limited residence time can be quantified by considering a situation where the turbulence field is homogeneous over the water depth, as can be realized in a settling column, for example. The mean residence time T_r for all particles in the water column with initial height Z_0 above the bottom of the water column can be obtained from:

$$\int_0^{T_r} W_s\,dt=\alpha''\int_0^{T_r} D_f^{n_f-1}\,dt=Z_0 \tag{8}$$

in which W_s is the settling velocity and $\alpha''=\alpha' g\Delta D_p^{3-n_f}/\nu$, where we have used fractal theory (e.g. Winterwerp, 1998):

$$W_s=\frac{\alpha}{18\beta}\frac{(\rho_s-\rho_w)g}{\mu}D_p^{3-n_f}\frac{D_f^{n_f-1}}{1+0.15Re_f^{0.687}}=\alpha'' D_f^{n_f-1} \tag{9}$$

assuming the particle (floc) Reynolds number Re_f is small. We can solve Eq. (1) (c.q. Eq. (7)) analytically if $q=0.5$ ($m=1$ and $n_f=2$) and for $q=0.5$ and $2n_f$ is an integer, using Eq. (8). For $n_f=2$ and 2.5 we find:

$$D_{T_r}=\frac{D_e}{1+\left(\frac{D_e}{D_0}-1\right)\exp\left\{-\frac{k_B Z_0 G^{3/2} D_e}{\alpha'' n_f}\right\}}\approx \tag{10a}$$

$$=D_e\left[1-\frac{D_e-D_0}{D_0}\exp\left\{-\frac{k_B Z_0 G^{3/2} D_e}{\alpha'' n_f}\right\}+\cdots\cdots\right]= \tag{10b}$$

$$=D_e\left[1-\frac{D_e-D_0}{D_0}\exp\left\{-\frac{k_A c G Z_0}{\alpha'' n_f}\right\}+\cdots\cdots\right]\quad \text{for } n_f=2$$

and

$$D_{T_r}=D_e\left[1-\frac{D_e-D_0}{D_e}\exp\left\{-\frac{k_B Z_0 G^{3/2}}{\alpha'' n_f}\right\}\right]\quad \text{for } n_f=2.5 \tag{11}$$

where D_0 is the initial floc size at $t=0$, not necessarily equal to D_p. Eq. (1) cannot be solved analytically for other values of n_f. As all analytical solutions have the same appearance as Eqs. (10b) and (11), we infer that a general form of the solution to Eq. (1) can be written as:

$$D_{T_r}=D_e-k_2(D_e-D_0)\exp\left\{-\frac{k_1 k_B G^{3/2} Z_0}{\alpha'' n_f}\right\} \tag{12}$$

in which k_1 and k_2 are coefficients to be determined. We can interpret D_{T_r} as the maximum floc size that can be attained in the time period that the flocs reside in a turbulent field with spatial dimensions characterized by Z_0, i.e. $D_{T_r}=D_{max}$. A characteristic length scale for Z_0 is the water depth h. The initial floc size D_0 can be interpreted as the smallest floc size to be found in the water column, occurring at reference conditions. Together with Eqs. (2) and (3), Eq. (12) becomes:

$$D_{max}=\frac{k_A c^{1/2q}}{k_B G^{1/2}}-k_2\left(\frac{k_A c^{1/2q}}{k_B G^{1/2}}-D_0\right)\exp\left\{-\frac{k_1 k_B G^{3/2} Z_0}{\alpha'' n_f}\right\}. \tag{13}$$

The concentration c should be interpreted as a characteristic value in the water column, for which the depth-mean

concentration is an obvious choice. Further, as $G \propto u_*^{3/2}$ and $\tau \propto u_*^2$, we use the following approximation: $G \propto \tau^{3/4}$. So we obtain a four-parameter formula in which the coefficients k_2, k_3, k_4 and n_f have to be determined empirically from field data (N.B. $k_2 \approx 1$ and $1 \leq n_f \leq 3$), assuming that $Z_0 \propto h$:

$$D_{max} = k_4 \frac{c^{1/2q}}{\tau^{3/8}} - k_2 \left(k_4 \frac{c^{1/2q}}{\tau^{3/8}} - D_0 \right) \exp\left\{ -\frac{k_3 \tau^{9/8} h}{n_f} \right\} \qquad (14)$$

in which τ (z, t) is the local shear stress in the water column. With the use of Eq. (8), Eq. (14) can also be written as:

$$W_{s,max} = \left[k_4 \frac{c^{1/2q}}{\tau^{3/8}} - k_2 \left(k_4 \frac{c^{1/2q}}{\tau^{3/8}} - \alpha'' D_0 \right) \exp\left\{ -\frac{k_3 \tau^{9/8} h}{n_f} \right\} \right]^{n_f - 1}. \qquad (15a)$$

The equilibrium settling velocity $W_{s,e}$ is given in Eq. (15b) and is obtained for large h and/or τ:

$$W_{s,e} = k_5 c^m \tau^{-3/8(n_f - 1)}. \qquad (15b)$$

Formula (15a) describes the settling velocity in high-energetic aquatic systems, such as estuaries and coastal seas where flocculation is driven primarily by physical parameters such as shear stress and SPM concentration, and the flocculation time is sufficiently small to observe variations in floc size over the tidal period. Organic matter and biological activity will affect the sticking efficiency of the flocculation process and their effect has to be accounted for in the model coefficients (in particular n_f and k_B). This model contains the hydro-sedimentological parameters h, τ and c, the floc property parameters D_0, m (c.q. q) and n_f and three empirical coefficients k_2, k_3 and k_4 that have to be obtained from data. Note that k_3 and k_4 are not non-dimensional and that their dimension depends on q and n_f. For a further physical description of these coefficients, see Sections 2.2 and 5.

2.2. Calibration of the flocculation model against Tamar

Manning (2001) collected a large data set on floc size and settling velocities in the Tamar estuary, located in the southern part of the UK. This estuary can be classified as mesotidal at neap tides, and macrotidal during spring conditions, with respective average tidal ranges of 2.2 and 4.7 m. Floc size measurements (Manning and Dyer, 2002a, see also Section 3.2.1 for description of methodology) were conducted in the upper reaches of the estuary near Calstock (which is about 30 km from the mouth) in a straight reach of the estuary within the tidal trajectory of the turbidity maximum. The mean depth at this measuring location amounts to about 3 m. Throughout the deployments τ and SPM concentrations, at the INSSEV sampling height, ranged from 0.04 to 0.7 Pa and 0.01 to 8.6 g l^{-1}, respectively. Of particular note was the observation of a concentrated benthic suspension (CBS) layer forming in the near-bed region at mid-tide periods during spring conditions. This created drag reduction at the lutocline and turbulence damping within the CBS layer, and in turn had a net influence on enhancing the flocculation process. This damping was observed by the time series from the EM current meter array, e.g. Dyer et al. (2002, 2004).

Peak macrofloc settling velocities of about 4–6 mm s^{-1} were observed within the CBS layers where SPM typically varied between 4–6 g l^{-1} and $\tau \sim 0.3$–0.36 Pa. Beyond 0.4 Pa, $W_{s,macro}$ values decreased rapidly in response to disaggregation as τ increased. For a sheared suspension of 4 g l^{-1}, a τ of 0.7 Pa led to a 33% decrease in $W_{s,macro}$. Above $\tau = 1.4$ Pa, $W_{s,macro}$ tended to decrease more slowly with increasing shear.

The Tamar experiments found that the proportion of macroflocs changed significantly across the turbidity maximum (Dyer et al., 2002). Before the passage of the turbidity maximum, the total floc mass tended to be equally divided between the macroflocs and microflocs on neaps, whilst on springs the macroflocs contributed 60–70%.

During the turbidity maximum passage at spring tide, macroflocs reached 2200 μm in diameter; these flocs had settling velocities of up to 16.6 mm s^{-1}. However, their effective densities were less than 50 kg m^{-3}, which means they would be prone to break-up when settling to a region of high shear. This large flocculation was produced by a combination of an SPM of 5.6 g l^{-1} and a τ of 0.36 Pa.

An abundance of fast settling macroflocs from spring tides meant they accounted for 83% of the time series averaged mass settling flux. Whereas during neap tides, the macroflocs contributed 15% less to the settling flux rate (Manning and Dyer, 2002a). This was partly due to a time series averaged macrofloc settling velocity of 3.9 mm s^{-1} from the spring tidal data; 2.1 mm s^{-1} higher than for neap tide conditions.

In our further analysis, we use macrofloc data only, as the macroflocs contribute most to the settling flux, owing to their large mass and faster settling velocities. Fig. 1 presents relations between the measured settling velocity and floc size and SPM concentration. From a fit based on power law regression through the first data set, a fractal dimension $n_f = 2.2$ is found (Winterwerp, 1998). A fit through the data in the right hand panel of Fig. 1 shows $m = 0.2$. It is noted that this value is much smaller than most observations reported in literature. Possibly, the higher values found elsewhere are caused by the sampling method deployed: if flocs are easily destroyed, only stronger, more dense flocs may be obtained during sampling. Part of these flocs may originate from bed erosion and a larger SPM concentration then is merely an indicator for larger flow velocities (and thus erosion of larger and stronger flocs) than that it affects the flocculation dynamics (see also Winterwerp et al., 2002). Note that the correlation coefficients for these fits are reasonable, bearing in mind that floc data always show very large scatter, and the fact that the floc size depends on other parameters as well.

Hence, four model parameters need to be tuned on the basis of our field data, as n_f and m have been determined independently from the data. Application of the model against the data showed immediately that k_2 should be unity, as for $k_2 \neq 1$, unrealistic results were obtained. This is encouraging as it implies that the analytical solutions given in Eqs. (10b) and (11) do not deviate too much from the best fit through

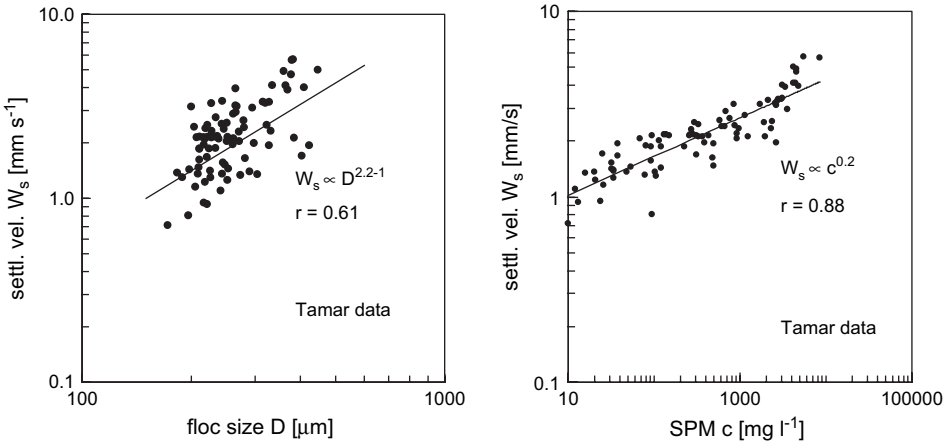

Fig. 1. Relation of settling velocity and floc size and SPM concentration measured in the Tamar estuary.

the data. The sensitivity to D_0 appeared to be small (see next section), and can be set to a realistic value without further tuning.

The solution to the flocculation equation suggests that the behaviour of the model at large τ is governed largely by k_4. This appeared indeed the case, and a little tuning of k_4 already resulted in proper agreement with the data for large τ; k_4 should be close to the ratio k_A/k_B, which was found to amount to about $\sim 10^{-3}$ in Winterwerp (1998). Then the final step was tuning k_3, as this coefficient determines the height and location of the maximum in the $W_s - \tau$ curves at smaller τ. Hence, the tuning of the coefficients appeared to be straightforward, and it was decided not to try to improve the fit with more advanced tools, such as multiple regression methods, as the scatter in the data themselves is so large that a much better fit is unlikely.

Fig. 2 presents a comparison of the flocculation equation (15a) with the coefficients from Table 1 with all macrofloc settling velocity data obtained in the Tamar estuary. The goodness of fit between model and data can be quantified with the absolute and relative standard deviation σ_{abs} and σ_{rel}, as defined below.

$$\sigma_{abs} = \sqrt{\frac{1}{N}\sum_{i}^{N}\left(W_{s,meas}(i) - W_{s,comp}(i)\right)^2} \quad \text{and}$$
$$\sigma_{rel} = \sqrt{\frac{1}{N}\sum_{i}^{N}\frac{\left(W_{s,meas}(i) - W_{s,comp}(i)\right)^2}{\left(W_{s,meas}(i)\right)^2}}. \tag{16}$$

The results are presented in Table 2 for all concentration ranges given in Fig. 2 and for all data as well. The relative standard deviation varies between 15 and 52%, with a mean value of 31%. We conclude that the model shows an excellent agreement over the full range of settling velocities ($0.5 < W_s < 5$ mm s^{-1} and $0.05 < c < 8$ g l^{-1}), again in relation to the scatter of the data themselves.

A final note concerns the value of the coefficient k_3. The value of k_3 is governed by k_B and a number of assumptions, such as the vertical gradient in turbulent shear stress, as in our heuristic flocculation formula we have assumed that the ratio of residence and flocculation time scale with water depth h.

2.3. Sensitivity analysis of the flocculation model

Next, the sensitivity of the flocculation equation (15a) to variations in its physical parameters is studied. The suspended sediment concentration is set to $C = 0.5$ g l^{-1} in all simulations, and all other parameters are set according to Table 1. Fig. 3a shows the effect of a limited residence time, in comparison to the equilibrium settling velocity. In shallow water, the residence time is so short that equilibrium floc size is only attained at fairly large shear rates ($\tau > 1.5$ Pa). With increasing water depth, equilibrium conditions are attained at much lower shear rates. At large h the equilibrium settling velocity is found.

Fig. 3b shows that the flocculation equation is not very sensitive to variations in the initial particle size. Also the

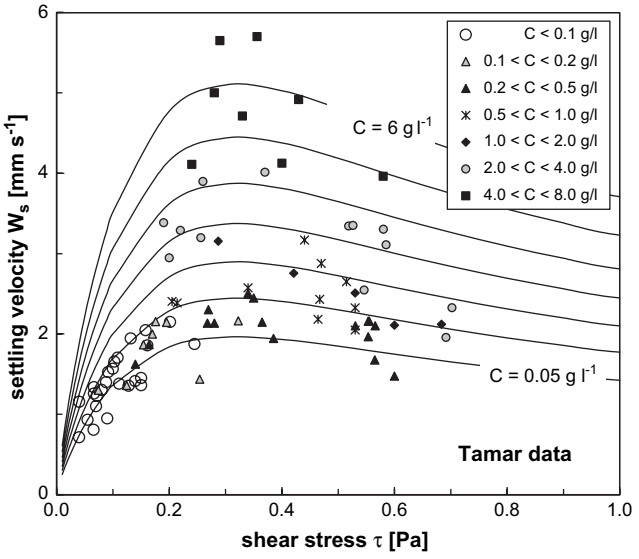

Fig. 2. Comparison flocculation equation (solid lines for $C = 0.05$; 0.15; 0.35; 0.75; 1.5; 3.0; and 6.0 g l^{-1}) with Tamar data.

Table 1
Coefficients in flocculation Eq. (15a) based on Tamar data

	n_f	k_2	k_3	k_4	D_0 (μm)	m	h (m)
Tamar	2.2	1	5	.007	10	0.2	3
Scheldt	2.15	1	5	.007	10	0.44	15

sensitivity to variations in m, i.e. the concentration-dependency of the equilibrium settling velocity is not very large (Fig. 3d). Even if this coefficient is set to a much larger value, i.e. $m = 1$, which is a value frequently mentioned in literature, the settling velocity appears to decrease by about 50% only.

The sensitivity of the flocculation equation to variations in floc structure, i.e. n_f, however, is large, in particular for values below $n_f = 2$ (Fig. 3c). This is due, of course, to the fact that n_f directly describes the specific density of the flocs and therefore appears in the power of the flocculation equation. This is an important observations, as the fractal dimension may vary considerably at one location. For example, Dyer and Manning (1998) reported a wide range in fractal dimensions for flocs observed in the Dollard estuary (The Netherlands). On the other hand, n_f can be determined from the relation between the settling velocity and particle size independently, which serves the applicability of the flocculation equation. Note that the proposed model can deal with one fractal dimension only.

3. Field campaign in the Lower Sea Scheldt

3.1. Site description

The drainage basin of the Scheldt river covers an area of nearly 22,000 km^2 and is situated in the northeast part of France, the west part of Belgium and the southwest part of The Netherlands (Fig. 4). The tide in the estuary is semi-diurnal. The tidal wave penetrates the estuary up to Gentbrugge, 156 km inland from the mouth. The mean tidal range is 3.85 m at the mouth and increases up to 5.24 m at Schelle (91 km from mouth). The average freshwater discharge is about 100 m^3 s^{-1}, with extreme values ranging between 20 m^3 s^{-1} during summer and 600 m^3 s^{-1} during winter (Belmans, 1988). The salinity in the river is variable, the main factors are the daily variation in tides, the spring–neap cycle and the freshwater discharge of the river. Wollast and Marijns (1981) have shown that the turbidity maximum of the estuary is situated at 110 km from the mouth during dry periods with low freshwater discharges, and at 50 km from the mouth at periods with high freshwater discharges. Salinity values range from 32 at the mouth to zero at Schelle.

Short waves are not important in the Lower Sea Scheldt, but occasionally on the intertidal areas, as the major part of the river is quite deep, and swell from the North Sea cannot propagate far enough.

An extensive measuring campaign was carried out in 2004 and 2005, using a number of survey vessels, anchored platforms and continuous measurements from fixed monitoring stations. The INSSEV measurements were carried out between February 17 and 19, 2005. Two different measurement locations were designated for the INSSEV (e.g. Section 3.2) measurement campaign: near the future Deurganckdok and near the entrance channel to the Kallo Lock as shown in Fig. 4. Both locations were near the bank of the river, out of the navigation channel, so as not to disturb the measurements by naval traffic. The campaigns were carried out in a spring to neap period at a tidal range of about 4.5 m.

3.2. Methodology

Flocs, although stable in flowing turbulent water, are easily destroyed when sampled owing to the shear created during acquisition (Eisma et al., 1997). Therefore, Scheldt floc data were acquired using the INSSEV, version 3.1 (Manning and Dyer, 2002a,b). INSSEV has the distinct advantage of permitting the simultaneous in-situ measurement of individual floc size and settling velocity, which permits accurate estimates of floc effective density and floc mass. The sampling apparatus comprises a two chamber device, with an integral underwater video camera, which views the flocs as they settle within a lower settling chamber. In the upper chamber, sediment-laden water is caught. Then this chamber is closed and the lower chamber is opened to allow flocs settling in still water. To prevent any vertical or horizontal motion during sampling, the INSSEV was secured to a heavy bed frame, which permitted Eulerian floc data sampling at a nominal height of 0.65 m above the bed.

In order to characterize the near-bed hydrodynamics, a Nortek 3-D Vector model 4229 acoustic Doppler velocity meter (ADV) was positioned alongside the INSSEV instrument. The ADV sensor (with integral pressure transducer) was attached to a vertical aluminium pole, which was laterally off-set from the INSSEV sampling unit, enabling detailed measurements of near-bed hydrodynamics at the INSSEV sampling height. The ADV's underwater electronics unit was specially adapted to accept the analogue connection of two miniature optical backscatter sensors (OBS). These turbidity probes were used to measure variations in the SPM concentration. The two OBS were also attached to the pole; one at the INSSEV sampling height and the other 0.4 m above the bed.

Table 2
Statistics of model performance for Tamar data (see Eq. (16) for definitions)

Conc. range	<0.1	0.1–0.2	0.2–0.5	0.5–1.0	1.0–2.0	2.0–4.0	4.0–8.0	All data
σ_{abs} (mm s^{-1})	0.23	0.45	0.72	0.80	1.20	1.11	0.64	0.69
σ_{rel} (%)	17	31	39	35	52	44	15	31

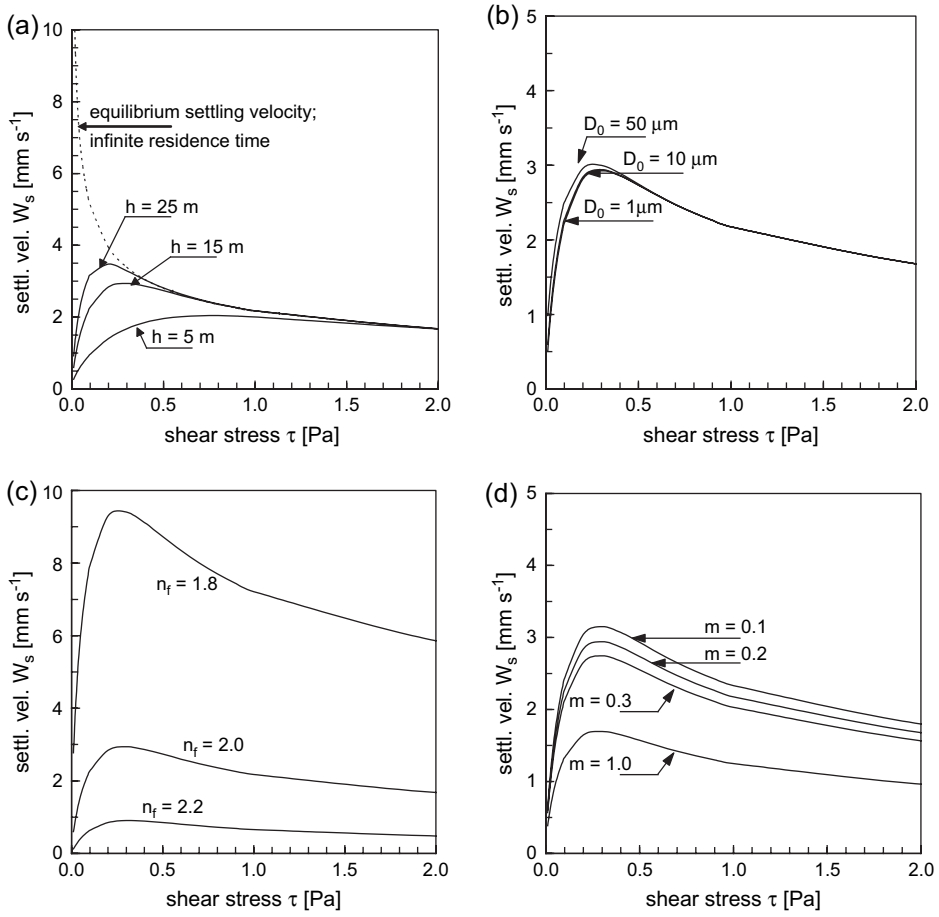

Fig. 3. Sensitivity of the flocculation equation to variations in water depth h, primary particle size D_0, fractal dimension n_f and concentration-dependency m for Table 1 settings and $C = 0.5\ \mathrm{g\,l^{-1}}$.

The flocculation measurements were conducted from the Dredging International workboat *Dommel*, which was securely moored fore and aft to specially deployed buoys at each survey site. All surface electronics and INSSEV recording systems were housed in the laboratory of the *Dommel*. Vessel position and logger time synchronization was established from a portable GPS units. Once the combined INSSEV, ADV and OBS rig had been deployed satisfactorily, the frame remained on the river bed for the entire acquisition duration (apart to undertake occasional instrument checks). To prevent turbulent vortices forming at the open ends of the INSSEV stilling chamber, the rig was aligned to within $\pm 5^\circ$ with the dominant flow direction. Instrumentation alignment was achieved by the inclusion of a 1.5×1.2 m high marine plywood rudder attached to the rear of the bed frame. The ADV's internal fluxgate compass and dual-axis tilt sensor provided an orientation reference frame for the hydrodynamic data.

INSSEV collected a representative floc population data set every 10–25 min (sampling frequency being a function of both the suspended sediment concentration and the slowest floc settling velocities of each population). Through-depth vertical profiles of salinity and temperature were obtained at approximately 30–45 min intervals using a Seabird Systems Seacat SBE 19-03 CTD, together with a Downing OBS to measure turbidity. Niskin bottle water samples were taken 65 cm above the bed every 30 min for OBS calibration and floc concentration referencing. Additional optical backscatter sensor calibrations were undertaken on the survey vessel's deck at the end of each day. Niskin water samples were decanted into pre-washed LDPE Nalgene bottles, which were stored in cooler boxes. The filtration of water samples was completed post-survey in the University of Plymouth's Ocean Science laboratory.

3.2.1. Data processing

The observed INSSEV floc images were recorded using an S-VHS unit and this provided the individual floc size D and settling velocity W_s data. All flocs observed for each population were analysed. The majority of the flocs were settling within the viscous Reynolds regime (i.e. when the Reynolds number, $Re_f < 0.5$), which meant the floc effective density could be determined by Stokes' law. For the exceptions where $Re_f > 0.5$, the Oseen correction (Schlichting, 1968) was applied to Stokes' law. All floc sizes reported in this paper are spherical equivalent, unless otherwise stated. Computational techniques derived by Fennessy et al. (1997), were then applied to calculate individual floc dry mass, porosity and the mass settling flux (MSF) distributions for each INSSEV floc sample. Further details of the floc data

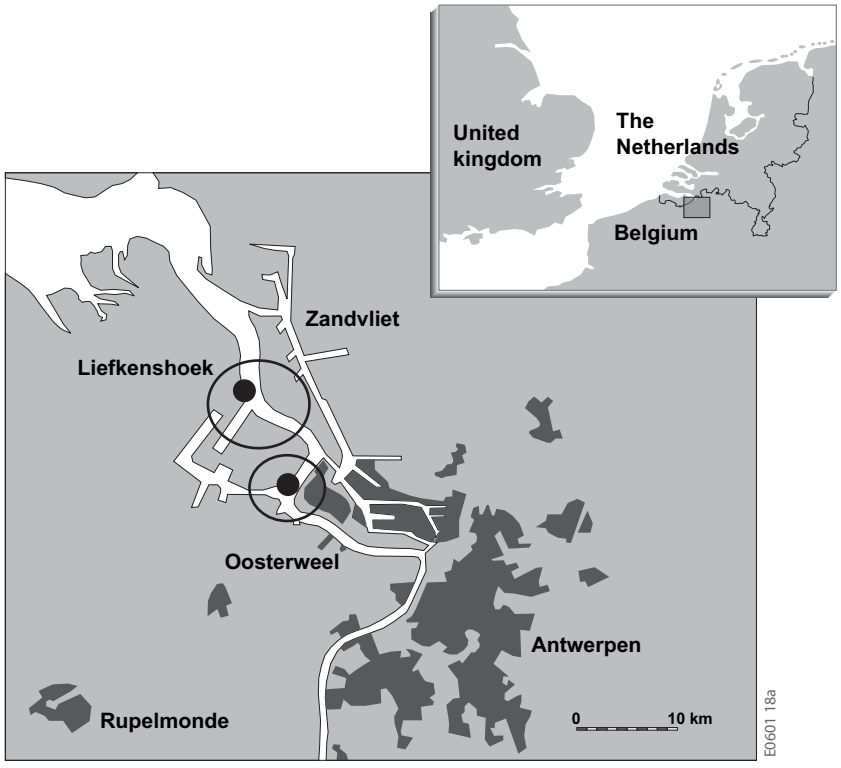

Fig. 4. Plan view of the Scheldt with survey areas (black dots).

processing are provided by Manning (2004a). Fractal dimensions were calculated with a formula by Winterwerp (1998).

The ADV and OBS sensors produced a continuous record of velocity and turbidity. Each time series was broken down into individual digital files of 5 min duration to enable the calculation of turbulent flow characteristics. At an acquisition rate of 32 Hz, this equates to an individual ADV file covering 9600 consecutive data points per channel. Once the raw files were de-multiplexed, Reynolds (1895) classic statistical decomposition of unsteady flow was applied to each data file and used to separate the turbulent fluctuating components from the burst-mean value. The deviations from the mean taken over each file's duration define the turbulent velocity components. Calculated variances of turbulence can be affected by spurious data spikes and non-stationarity of the time series. Spikes were identified by detrending the time series data using a linear fit, and then replacing variations greater than three times the standard deviations with an interpolated value (French and Clifford, 1992).

The resulting detrended and despiked time series were then used to calculate the velocity variances and the turbulent velocity values. The turbulent shear stresses were calculated from the total turbulent kinetic energy, as it is much less sensitive to instrumentation alignment than the Reynolds stress approach (Heathershaw, 1979). Burst-averaged values of turbulent kinetic energy (e.g. Stapleton and Huntley, 1995) were calculated for each 5 min duration data file. The turbulent shear stress τ is proportional to the turbulent kinetic energy (Soulsby, 1983), by assuming energy production equals energy dissipation (Nakagawa and Nezu, 1975).

3.3. Lower Scheldt estuary results

3.3.1. Hydrodynamics

Measurements were conducted near neap tidal conditions in the Deurganckdok vicinity of the Lower Scheldt estuary. The water column was 17.3 m deep at high water (HW) with a constant temperature of 5.8 °C. This was approximately 4.8 °C warmer than the on-deck air temperature. As the ebb tide moved to low water, the water column temperature increased by 0.4 °C. The upper 0.5 m of the water column was significantly colder than the remainder, registering temperatures ranging from 2.5 to 4 °C. A surface salinity of 3.7 was measured at HW, whilst the near-bed salinity was 1 higher. The observed colder surface water corresponded with patches of freshwater. By LW, the salinity of the 12.5 m deep water column had fallen to a homogeneous 1.4.

A turbidity maximum (ETM) was observed at the sampling location just after local HW. The ETM displayed SPM concentrations of 150–300 mg l^{-1} in the region 2 m above the river bed and remained in the Deurganckdok location for just over an hour. Outside of the ETM zone, SPM concentration was predominantly under 100 mg l^{-1} through to mid-ebb, and this then halved by LWS.

The along-stream current velocity U record showed the near bed (65 cm) velocity slowing in the latter stages of the flood from 0.11 m s^{-1} and becoming momentarily stationary at HW. From then on the tide reversed to ebb direction. The flow steadily accelerated to an ebb velocity peak of 0.7 m s^{-1}. The flow varied between 0.4 and 0.7 m s^{-1} during the mid-tide period, before starting to decelerate towards LWS. As one would

expect U was the dominant flow component. The across-stream velocity, V, was seen to fluctuate between 0.05 and 0.23 m s^{-1} during the mid-tide period, whilst the vertical flow, W, rarely exceeded 0.1 m s^{-1} throughout the entire sampling period. As said, waves are not important in this part of the estuary.

3.3.2. Time series of floc size

Fig. 5a shows the time series for variations in SPM concentration and turbulent shear stress, at the INSSEV sampling height of 0.65 m above the river bed, for the neap tide survey conducted on February 17, 2005, together with the variation in water level (add 12 m to get total water depth). The deployment continuously covered the last part of the flood and on through the ebb to LWS, and then the early part of the following flood. A total of 21 INSSEV floc samples were collected on this survey day. The corresponding distribution of sample mean spherical-equivalent floc size D_{mean} and mean settling velocity $W_{\text{s,mean}}$, both of which are dry floc mass weighted means, are illustrated in Fig. 5b.

The shear stress τ increased from 0.24 Pa, observed within the turbidity maximum just after HW, up to 1.5 Pa by mid-ebb. The mean size of the flocs responded by reducing from

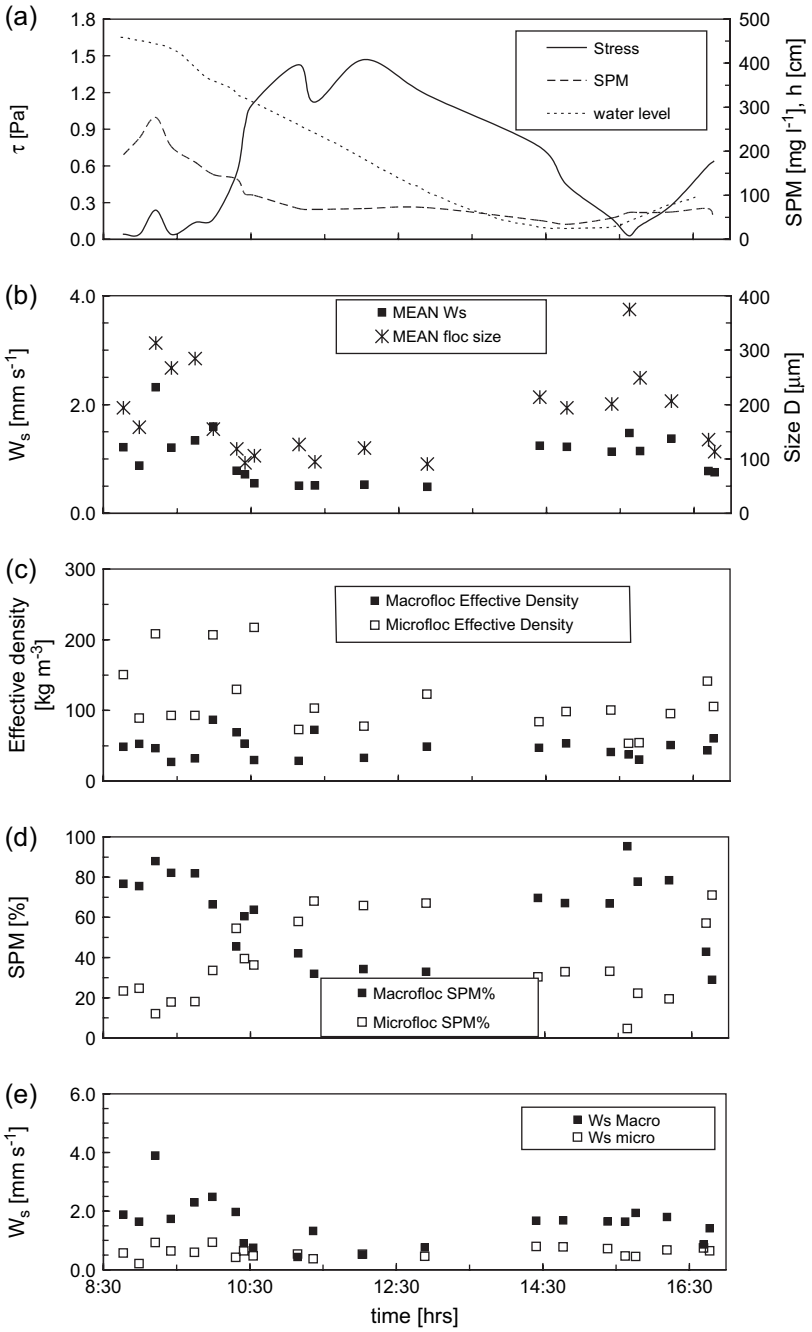

Fig. 5. Time series of floc properties for February 17, 2005. (a) Shear stress τ, SPM and water level h; (b) mean floc size D_{mean} and settling velocity W_s; (c) macrofloc and microfloc effective density; (d) macrofloc and microfloc SPM distribution; and (e) macrofloc and microfloc settling velocity.

313 μm down to less than 100 μm in the same time frame. Similarly, $W_{s,mean}$ reduced by nearly an order of magnitude during the early ebb from an initial turbidity maximum settling velocity of 2.3 mm s^{-1}.

As low water approached and the flow velocity slowed, the lower stress permitted D_{mean} to grow to 200 μm, and these flocs settled at $W_{s,mean} \approx 1.1-1.2$ mm s^{-1}. As the tide turned, so the shear stress and SPM conditions returned to those more favorable for flocculation. The mean floc size at the early part of the flood increased by 25–87% to 250–375 μm, whilst their average settling velocity suggests these flocs fell nearly 20% quicker ($W_{s,mean} = 1.4$ mm s^{-1}).

Whilst the sample-averaged floc characteristics indicate general trends, the macrofloc and microfloc properties identify more discrete details about the dynamics of the settling floc population. Manning (2001) defines the critical size between these two fractions as 160 μm, and the macrofloc and microfloc properties were determined from each complete INSSEV floc population spectrum. Fig. 5c and d show the effective density and SPM distribution, respectively, of all flocs within the macrofloc and microfloc sub-populations. The denser microflocs, with mean ρ_e values reaching 217 kg m^{-3}, tended to dominate the suspended matter characteristics during the first half of the ebb conditions and these comprised 35–68% of the SPM. From floc size and density, floc porosity can be obtained, showing that these dense microflocs were 80–90% porous and had settling velocities of 0.4–0.6 mm s^{-1} (Fig. 5e), whereas in the ETM zone, the faster settling macroflocs ($W_{s,macro} = 3.9$ mm s^{-1}) represented 75–88% of the floc mass. The majority of these large flocs were highly porous, comprising an average of 95% voids, and this was reflected in their effective densities being less than 50 kg m^{-3}.

The sample average macrofloc sizes for all Lower Scheldt estuary samples ranged between 175 and 580 μm. $W_{s,macro}$ peaked at 3.9 mm s^{-1}, although the majority are under 2 mm s^{-1}.

Fig. 6 shows the variation of all settling velocity data (macroflocs only) with floc size D and SPM concentrations. It is shown that an average n_f value of 2.15 is found from linear regression, and that the variation of W_s with c is again fairly small, but larger than for the Tamar estuary, i.e. $W_s \propto c^{0.44}$. Note that the regression coefficients are not too large.

3.3.3. Spectral floc observations

Within the turbidity maximum zone, the SPM concentration was 277 mg l^{-1} at 0.65 m above the bed and remained in excess of 240 mg l^{-1} for a 20-min period during the passage of the turbidity maximum. The floc distribution of sample 3-17D, illustrated in Fig. 7a shows a bi-modal population. The first mode was composed of microflocs up to 150 μm in diameter and represented a fifth of the total population. This sub-population was dominated by compact, moderately dense ($\rho_e = 150-470$ kg m^{-3}) flocs characterized by fractal dimensions of 2.4–2.7.

The remaining 80% of the ETM floc population were large macroflocs with an average diameter of 507 μm. These macroflocs had individual settling velocities ranging from 1 to 11 mm s^{-1}. In the ETM the macroflocs represented 88% of the floc mass and had a $W_{s,macro} = 3.9$ mm s^{-1}, representing 75–88% of the floc mass. In terms of mass settling, the macroflocs contributed to 97% of the total settling flux.

A peak near-bed ebb current velocity of 0.7 m s^{-1} was attained just 2 h after high water (HW) with peak turbulent shear stresses, and Fig. 7b illustrates the floc size and settling velocity distribution of the representative sample 10-17D. Further analysis of 10-17D showed that of the total 70 mg l^{-1} SPM concentration, the floc mass distribution was now weighted 58:42 in favour of the microflocs. The microflocs had a fractal dimensions ranging from 2.14 to 2.2; this compared to n_f values of 1.8–1.9 for the larger macrofloc fraction. This was a reflection of the microflocs effective densities, generally being an order of magnitude greater than that of the macroflocs.

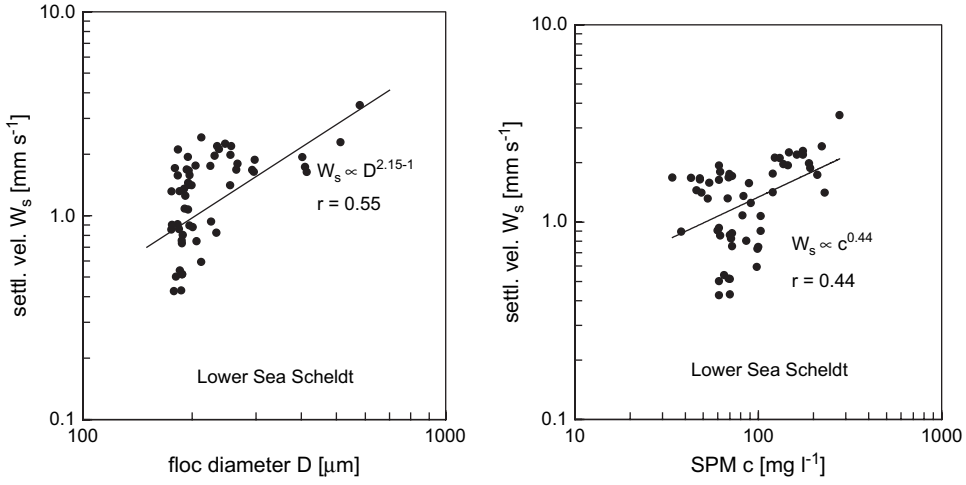

Fig. 6. Relation of settling velocity and floc size and SPM concentration measured in the Lower Sea Scheldt estuary.

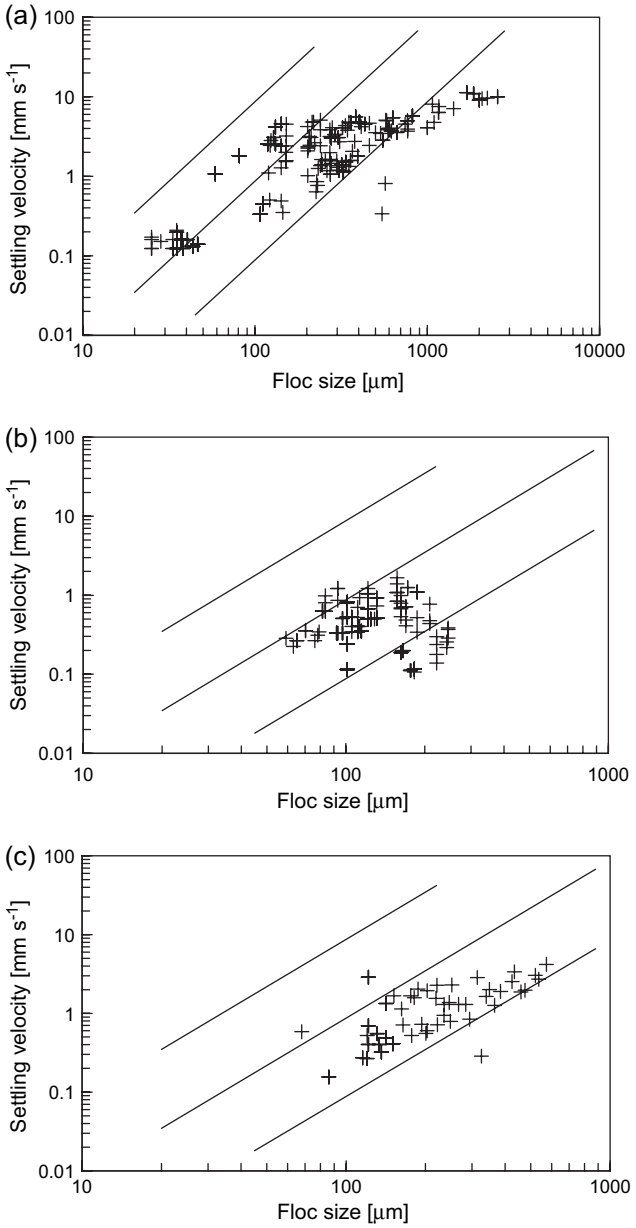

Fig. 7. W_s vs D for Scheldt estuary floc samples: (a) sample 3-17B; (b) sample 10-17D; and (c) sample 16-17D. Lines indicate constant effective densities (i.e. 16, 160 and 1600 kg m^{-3}).

The denser microflocs were only 80–85% porous. The $W_{s,macro}$ was 0.43 mm s^{-1}, which was 0.1 mm s^{-1} slower than the microfloc fraction. In terms of the total mass settling flux, the microflocs now contributed 63%.

During LWS the SPM concentration had reduced to only 48 mg l^{-1}. The 75 flocs of sample 16-17D (Fig. 7c) settled at velocities ranging from 0.16 to 4.2 mm s^{-1}. In contrast to the turbidity maximum, where macroflocs were abundant, beyond 400 µm, the number of 16-17D macroflocs exponentially decreased with increasing size. Generally, floc effective densities were less than 160 kg m^{-3}, whilst fractal dimensions tended to range from 2.1 to 2.2. In comparison, both slack water and ETM populations (3-17D) comprised individual macrofloc to microfloc ratios of 0.8 to 1. However, when the relative macrofloc to microfloc SPM concentration ratios are examined, the macrofloc mass was two times larger than the microfloc mass at slack water. Whilst ETM environment permitted this ratio to rise by a further 5.3 in favour of the macroflocs (SPM ratio of 7.3 to 1). The slack water $W_{s,macro}$ was only 1.6 mm s^{-1}, which was two and a half times slower than the ETM sample. In terms of mass settling flux (MSF), the macroflocs contributed 83% of the total slack LW flux (MSF = 72 mg m^{-2} s^{-1}), which was 14% less than within the ETM zone.

4. Application of the flocculation model to Lower Sea Scheldt data

In this section we apply the heuristic flocculation formula and model parameters k_2, k_3, k_4 and D_0 from Table 1, as obtained from calibration of the model against data from the Tamar estuary, to the data of the Lower Scheldt estuary. We use the results of Fig. 6, i.e. $n_f = 2.15$ and $m = 0.44$; the water depth is set at its local value $h = 15$ m. These parameters are summarized in Table 1 for convenience.

Fig. 8 shows a comparison of the model predictions and the data. Table 3 presents the goodness of fit, showing a relative standard deviation for the three SPM-classes varying between 40 and 56% with a mean of about 50% for all data. Though the data show quite some scatter, the agreement between predictions and observations is satisfactory. Note that the variation in SPM concentration is much smaller than in the Tamar estuary.

5. Discussion and conclusions

We have carried out new series measurements of the settling velocity of cohesive sediment flocs in the Lower Sea Scheldt, Belgium, and compared the data with the results of earlier measurements in the Tamar estuary. These rivers are situated in temperate climate zone, and are fairly dynamic in

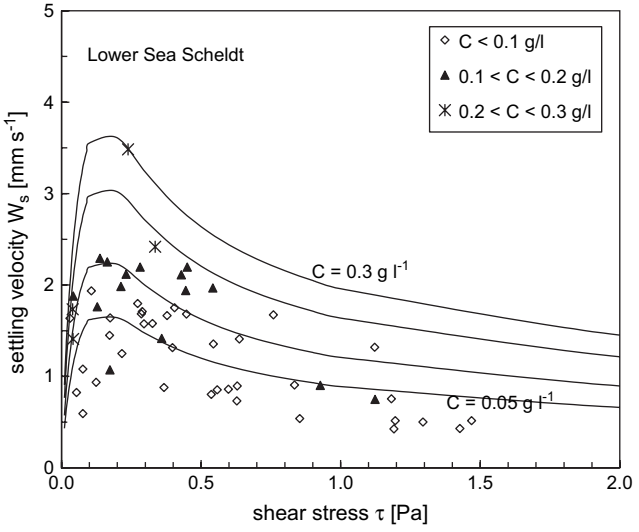

Fig. 8. Comparison flocculation equation (solid lines for $C = 0.05$; 0.1; 0.2 and 0.3 g l^{-1}) with Lower Sea Scheldt data.

Table 3
Statistics of model performance for Lower Sea Scheldt data (see Eq. (16) for definitions)

Conc. range	<0.1	0.1–0.2	0.2–0.3	All data
σ_{abs} (mm s^{-1})	0.39	0.66	0.64	0.50
σ_{rel} (%)	48	56	40	49

the sense that they are characterized by mesotidal conditions, high flow velocities and high turbidity. This is reflected by fairly dense flocs with large fractal dimensions, of about 2.2, which is characteristic for the so-called reaction limited regime of flocculation. In other words, variations in floc size are merely governed by the (local) hydrodynamic conditions (including the effects of high turbidity). The effects of biological activity (EPS and TEM) are to be accounted for in the floc structure (i.e. the fractal dimension n_f) and the sticking probability (i.e. the flocculation parameter k_A, i.e. k_4). It is noted that all estuaries are characterized by saline to brackish conditions; in the brackish zones, salinity is so large, however, that variations in salinity are not expected to affect the flocculation process.

It is also remarkable that the variation of floc size with SPM concentration is fairly small, consistently much smaller than earlier findings by e.g. Thorn (1981), Ross (1988), and Wolanski et al. (1992). We have no definite explanation for this observation, but it might be due to developments in measuring techniques, in particular the way of floc sampling. The current INSSEV system allows for almost undisturbed sampling, keeping the flocs intact. Older methods do destroy flocs to a larger or lesser extend, in particular the more fragile ones. Hence, sampling may have been biased towards the stronger flocs, which are not formed in the water column, but originate from the river bed by erosion (larger flow velocity, more erosion of larger particles and higher SPM-values).

Next, we have developed a parameterization of an analytical solution of the Lagrangean flocculation equation derived by Winterwerp (1998). This model accounts for the variation in settling velocity of mud flocs in dynamic environments as a function of shear stress and suspended sediment concentration. We have also included the effects of a limited residence time of the flocs in the turbulent water column. This parameterization contains seven coefficients, two of which can be determined independently from plotting settling velocity data against floc size and SPM concentrations, i.e. the fractal dimension and the concentration-dependency of the settling velocity. The third physical parameter to be determined independently is the local water depth.

Four parameters had to be obtained through calibration of the model against field observations. One parameter appeared to be unity – other values resulted in completely unrealistic distributions. Furthermore, the results appeared to be fairly insensitive to the size of primary particles. The two remaining parameters can be obtained by a two-step trial and error method. The value of these parameters appeared to be in the range to be expected from physical analysis.

The heuristic model is compared with data obtained in the Tamar estuary (UK), and The Lower Scheldt estuary (Belgium). The relative error of the predictions amounts to 30–50%. The observed values of floc size and settling velocity show a large scatter, even at comparable hydro-sedimentological conditions. With this limitation in mind, it can be concluded that the flocculation model predicts the observations in a satisfactory manner, well within the scatter of the data themselves. The model was also applied to a data obtained in the Gironde estuary, France (e.g. Manning et al., 2004), and again the model compared favorable with the data, with an overall standard deviation of about 30%. However, the maximum in W_s was not exactly predicted at the proper shear stress. Because of limited space, we cannot present the results here.

This flocculation model is developed to be implemented in three-dimensional sediment transport models, as the use of a full time-dependent flocculation model (either Lagrangean or Eulerian) is prohibitive from a computational time point of view. This is ongoing work and the first results are to be expected by mid-2006. Hence, it is too early to conclude whether this approach works. It is noted that the model (15a) uses the shear stress as independent parameter. In a three-dimensional sediment transport model it may be advisable to use the turbulent kinetic energy k instead, as τ may become zero, whereas k maintains positive values in advanced turbulence closure models.

It is promising that the model predicts settling velocities in three different estuaries to the right order of magnitude, changing only three physical parameters that can be obtained from an independent analysis of settling velocity data. We believe that this is owed to the fact that the model is based on a physical concept that yielded fair results (Winterwerp, 2002). In that sense, the new heuristic flocculation model can be considered to be an improvement on the fully empirical models developed by for instance Van Leussen (1994) and Manning (2004c).

Acknowledgements

We like to thank Ministry of the Flemish Community (Ministerie van de Vlaamse Gemeenschap) for the funding of the project, and their permission to publish the results. Staff from ms Zeeschelde and Gems International are acknowledged for the good collaboration during the field measurements. Finally, Dr. Ken Kingston (University of Plymouth) is acknowledged for his assistance with the initial stages of the model calibration.

References

Belmans, H., November 1988. Capital and maintenance dredging in Western and Sea Scheldt. Tijdschrift Water (in Dutch).

Droppo, I.G., Leppard, G.G., Liss, S.N., Milligan, T.G., 2005. Flocculation in Natural and Engineered Environmental Systems. CRC Press, Florida.

Dyer, K.R., 1989. Sediment processes in estuaries: future research requirements. Journal of Geophysical Research 94 (C10), 14327–14339.

Dyer, K.R., Manning, A.J., 1998. Observation of the size, settling velocity and effective density of flocs, and their fractal dimensions. Journal of Sea Research 41, 87–95.

Dyer, K.R., Bale, A.J., Christie, M.C., Feates, N., Jones, S., Manning, A.J., 2002. The turbidity maximum in a mesotidal estuary, the Tamar Estuary, UK. Part II: the floc properties. In: Winterwerp, J.C., Kranenburg, C. (Eds.), Fine Sediment Dynamics in the Marine Environment – Proceedings in Marine Science, 5. Elsevier, Amsterdam, pp. 219–232.

Dyer, K.R., Christie, M.C., Manning, A.J., 2004. The effects of suspended sediment on turbulence within an estuarine turbidity maximum. Estuarine, Coastal and Shelf Science 59, 237–248.

Eisma, D., Dyer, K.R., van Leussen, W., 1997. The in-situ determination of the settling velocities of suspended fine-grained sediment – a review. In: Burt, N., Parker, R., Watts, J. (Eds.), Cohesive Sediments – Proceedings of INTERCOH Conf. (Wallingford, England). John Wiley & Son, Chichester, pp. 17–44.

Fennessy, M.J., Dyer, K.R., Huntley, D.A., 1994. INSSEV: an instrument to measure the size and settling velocity of flocs in-situ. Marine Geology 117, 107–117.

Fennessy, M.J., Dyer, K.R., Huntley, D.A., Bale, A.J., 1997. Estimation of settling flux spectra in estuaries using INSSEV. In: Burt, N., Parker, R., Watts, J. (Eds.), Cohesive Sediments – Proceedings of INTERCOH Conf. (Wallingford, England). John Wiley & Son, Chichester, pp. 87–104.

French, J.R., Clifford, N.J., 1992. Characteristics and event structure of near-bed turbulence in a macro-tidal saltmarsh channel. Estuarine, Coastal and Shelf Science 34, 49–69.

Heathershaw, A.D., 1979. The turbulent structure of the bottom boundary layer in a tidal current. Geophysical Journal of the Royal Astronomical Society 58, 395–430.

Kranenburg, C., 1994. On the fractal structure of cohesive sediment aggregates. Estuarine, Coastal and Shelf Science 39, 451–460.

Krone, R.B., 1984. The significance of aggregate properties to transport processes. In: Estuarine and Cohesive Sediment Dynamics: Proceedings of a Workshop on Cohesive Sediment Dynamics with Special Reference to Physical Processes in Estuaries, Tampa, Florida. Lecture Notes on Coastal and Estuarine Studies, vol. 14. Springer Verlag, pp. 66–84.

Manning, A.J., 2001. A study of the effect of turbulence on the properties of flocculated mud. PhD thesis, Institute of Marine Studies, University of Plymouth, UK, 282 pp.

Manning, A.J., 2004a. Observations of the properties of flocculated cohesive sediment in three western European estuaries. Journal of Coastal Research 41 (Special Issue, SI), 90–104.

Manning, A.J., 2004b. The effects of turbulence on estuarine flocculation. Journal of Coastal Research 41 (Special Issue SI), 70–81.

Manning, A.J., 2004c. The Development of New Algorithms to Parameterize the Mass Settling Flux of Flocculated Estuarine Sediments. HR Wallingford Ltd, UK, Technical Report No. TR 145, 26 pp.

Manning, A.J., Dyer, K.R., 2002a. The use of optics for the in-situ determination of flocculated mud characteristics. Journal of Optics A: Pure and Applied Optics 4, S71–S81 (Institute of Physics Publishing).

Manning, A.J., Dyer, K.R., 2002b. A comparison of floc properties observed during neap and spring tidal conditions. In: Winterwerp, J.C., Kranenburg, C. (Eds.), Fine Sediment Dynamics in the Marine Environment – Proceedings in Marine Science, vol. 5. Elsevier, Amsterdam, pp. 233–250.

Manning, A.J., Dyer, K.R., Lafite, R., Mikes, D., 2004. Flocculation measured by video based instruments in the Gironde Estuary during the European Commission SWAMIEE project. Journal of Coastal Research 41 (Special Issue SI), 58–69.

Nakagawa, H., Nezu, I., 1975. Turbulence in open channel flow over smooth and rough beds. Proceedings of Japan Society of Civil Engineering 241, 155–168.

Reynolds, O., 1895. On the dynamical theory of incompressible viscous fluids and the determination of the criterion. Philosophical Transactions of the Royal Society 186A, 123–164.

Ross, M.A., 1988. Vertical structure of estuarine fine sediment suspensions. PhD-thesis, Coastal & Oceanographic Engineering Department, University of Florida, Gainesville, Florida, USA.

Schlichting, H., 1968. Boundary-layer Theory. McGraw-Hill, New York, 747 pp.

Soulsby, R.L., 1983. The bottom boundary layer of shelf seas. In: Johns, B. (Ed.), Physical Oceanography of Coastal and Shelf Seas. Elsevier, New York, pp. 189–266.

Stapleton, K.R., Huntley, D.A., 1995. Sea bed stress determinations using the inertial dissipation method and the turbulent kinetic energy method. Earth Surface Processes and Landforms 20, 807–815.

Thorn, M.F.C., 1981. Physical processes of siltation in tidal channels. In: Proceedings of Hydraulic Modelling Applied to Maritime Engineering Problems. ICE, London, pp. 47–55.

Van Leussen, W., 1994. Estuarine macroflocs – their role in fine-grained sediment transport. PhD-thesis, University of Utrecht, The Netherlands.

Vicsek, T., 1992. Fractal Growth Phenomena. World Scientific, Singapore.

Wolanski, E., Gibbs, R.J., Mazda, Y., Mehta, A.J., King, B., 1992. The role of turbulence in settling of mudflocs. Journal of Coastal Research 8 (1), 35–46.

Wolanski, E., Spagnol, S., Thomas, S., Moore, K., Alogni, D.M., Davidson, A., 2000. Modelling and visualizing the fate of shrimp pond effluent in a mangrove-fringed tidal creek. Estuarine, Coastal and Shelf Science 50, 85–97.

Winterwerp, J.C., 1998. A simple model for turbulence induced flocculation of cohesive sediments. IAHR. Journal of Hydraulic Research 36 (3), 309–326.

Winterwerp, J.C., 2002. On the flocculation and settling velocity of estuarine mud. Continental Shelf Research 22, 1339–1360.

Winterwerp, J.C., Bale, A.J., Christie, M.C., Dyer, K.R., Jones, S., Lintern, D.G., Manning, A.J., Roberts, W., 2002. Flocculation and settling velocity of fine sediment. In: Winterwerp, J.C., Kranenburg, C. (Eds.), Proceedings in Marine Science, No 5; Proceedings of the 6th International Conference on Nearshore and Estuarine Cohesive Sediment Transport. Elsevier, pp. 25–40. INTERCOH-2000.

Winterwerp, J.C., Van Kesteren, W.G.M., 2004. Introduction to the physics of cohesive sediments in the marine environment. In: Developments in Sedimentology, vol. 56. Elsevier.

Winterwerp, J.C., 2005. Equilibrium and non-equilibrium floc sizes – or: flocculation takes time. In: Droppo, I.G., Leppard, G.G., Milligan, T.G. (Eds.), Flocculation in Natural and Engineered Environmental Systems. CRC Press, pp. 249–270.

Wollast, R., Marijns, A., 1981. Evaluation des contributions de differentes sources de matières en suspension à l'envasement de l'Escaut, Final report to the Belgium Ministry of Public Health and Environment, 152 pp.